Depth-Independent Drag Force Induced by Stirring in Granular Media

François Guillard,* Yoël Forterre,† and Olivier Pouliquen‡
Aix-Marseille Université, CNRS, IUSTI UMR 7343, 13453, Marseille, France
(Received 24 October 2012; published 26 March 2013)

The drag force experienced by a horizontal cylinder rotating around the vertical axis in a granular medium under gravity is experimentally investigated. We show that, for deeply buried objects, the drag force dramatically drops after half a turn, as soon as the cylinder crosses its own wake. Whereas the drag during the first half turn increases linearly with the depth, the drag after several rotations appears to be independent of depth, in contradiction with the classical frictional picture stipulating that the drag is proportional to the hydrostatic pressure. We systematically study how the saturated drag force scales with the control parameters and show that this effect may be used to drill deeply in a granular medium without developing high torques.

DOI: 10.1103/PhysRevLett.110.138303 PACS numbers: 47.57.Gc, 45.20.da, 45.70.−n

In fluid mechanics, the problem of the forces experienced by an object moving in a fluid has been extensively studied. Whereas most investigations concern objects moving in a Newtonian fluid, the case of complex fluids attracts more and more interest. Drag forces in viscoelastic liquids like polymers [1] or in viscoplastic materials like clays, gels [2], or foams [3] have been studied and reveal unexpected phenomena. In this work, we consider the problem of the drag force on an object moving in a granular medium. Granular materials can be considered as a complex fluid and belong to the viscoplastic class of material [4]: a yield stress exists, meaning that the material behaves like a solid below a critical shear stress and flows above. The specificity of granular media is that the rheology is mainly controlled by a friction criterion: the shear stress is proportional to the confining pressure. The question of the forces exerted on an object moving in a granular material is of interest in many industrial and agricultural applications (mixing processing, blenders, soil plowing [5]), in geophysical problems, for example, for the design of snow obstacles [6] or for the modeling of impact cratering, and in some biomechanical problems concerning animal locomotion in sand [7] or plant-soil interactions [8]. Experimentally, different configurations have been studied. A first configuration is the plow: a vertical plate or a vertical cylinder is partially buried in the sand and is pulled horizontally [9–13]. Another configuration is the case of an object entirely buried in the granular material, which moves horizontally at a fixed depth in the medium [14–17]. A last case corresponds to the impact problem, when an object penetrates vertically the granular layer [18–24]. In all these situations, a rich phenomenology has been observed and the velocity dependence [9,16], the effect of the boundaries [20,25], and the existence of lift forces associated with the motion [17] have been studied. One major feature common to all the above configurations is the frictional scaling of the drag force in the limit of quasistatic motions. When the motion of the object is slow enough, the drag is found to be proportional to the ambient confining pressure times the surface of the object. For a wide enough container, the pressure is proportional to the depth. Therefore, an object moving in a granular medium under gravity experiences a drag force that increases linearly with the depth.

In this Letter, we study the torque needed to rotate around the vertical axis a cylinder buried inside a granular medium and report an unexpected phenomenon. The drag force on the cylinder dramatically drops after one turn and becomes independent of the depth, unlike the classical frictional scaling.

The experiment is sketched in Fig. 1. It consists of a horizontal cylinder in stainless steel immersed in a rotating bucket full of grains. The tank is 30 cm in diameter and rotates at a constant angular velocity $\Omega = 2$ rpm around its vertical axis. It is filled with 23 cm of glass beads with diameters between 500 and 530 μm. Cylinders of various sizes have been used with diameters D from 1.5 to 6 mm and lengths L between 1.5 and 12 cm. The cylinder is maintained horizontally in the granular bed at a controlled depth h (distance between the free surface and the axis of the cylinder) by a thin rigid vertical rod 3 mm in diameter, whose axis coincides with the rotation axis (Fig. 1). When the tank is put in rotation, the cylinder is kept static by the vertical rod and experiences a torque, which is measured at the top using a torque meter. To get information on the drag exerted on the horizontal cylinder only, the contribution of the vertical support is systematically subtracted from the total torque (its contribution is about 5% of the total torque). In order to compare the torque measurement $\mathcal{M}$ in our rotating device with the drag force one would measure when pulling the same object in a granular bed, we define the equivalent drag force F_{drag} as

$$F_{\mathrm{drag}} \equiv 4\mathcal{M}/L. \quad (1)$$

This relation simply comes from the assumption that each half of the rotating cylinder experiences half of the force

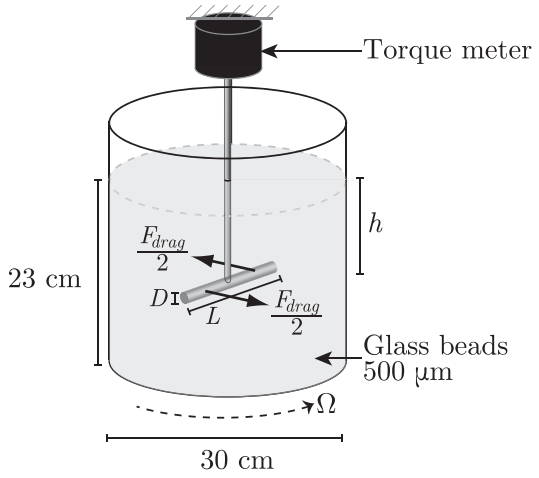

FIG. 1. Sketch of the experimental device.

F_{drag} one would measure when dragging the whole cylinder (Fig. 1). In the following, all our measurements are expressed in terms of F_{drag}. Note that our setup is similar to the one developed by Brzinski and Durian [16] who studied drag forces in various gravity and velocity conditions. However, an important difference is the depth of our container, which is larger than the length of the cylinder. We will see that this condition enables us to reveal a new unexpected regime.

The experimental procedure is the following. The packing is stirred vigorously and homogeneously and then slightly compacted by lateral taps on the tank. The estimated mean volume fraction at the beginning of the experiments is $\phi = 0.62$. The cylinder is then plunged at the desired depth into the granular medium and the tank is put in rotation while recording the torque. All the experiments have been carried out in the quasistatic regime (the inertial number is less than 5×10^{-3}), when the measured torque is independent of the angular velocity [9]. Typical time evolutions of the drag force on the cylinder are plotted in Fig. 2(a) for different depths h. When starting the rotation, the drag force rapidly increases, reaches a maximum, and drops. After several rotations, it eventually reaches a stationary value. The striking result is that, whereas the drag force during the first half-rotation increases with depth h, the stationary value after long time is roughly the same for all runs. This means that the higher the depth, the higher the drop of the drag force after several rotations. Figure 2(b) shows how the maximum drag force during the first half-rotation $F^{\mathrm{half}}_{\mathrm{drag}}$ and the stationary drag force after several rotations $F^{\infty}_{\mathrm{drag}}$ varies when changing the depth h of the cylinder. Whereas $F^{\mathrm{half}}_{\mathrm{drag}}$ increases linearly with h as expected from our knowledge of the frictional nature of the drag in granular media, $F^{\infty}_{\mathrm{drag}}$, which initially follows the same trend, rapidly saturates and becomes independent of h for $h > h_{\mathrm{crit}}$, with $h_{\mathrm{crit}} \simeq 6$ cm in this case. This saturation of the drag force with the depth is observed for all the cylinders we have tested, but the critical thickness and the level of saturation depend on the length of the object, a point we will discuss later. The measurements then show that the drag force after several rotations is independent of the hydrostatic pressure. Passing over and over in its own wake seems to create a structure within the packing, which is able to screen the mass of grains above and dramatically lower the force needed to move.

We have checked that this depth-independent steady drag is a robust phenomenon. First, the stationary value $F^{\infty}_{\mathrm{drag}}$ is independent of the preparation of the sample. Starting from a loose or a dense packing changes the drag during the first half-rotation but not its stationary value after several rotations. Similarly, first putting the

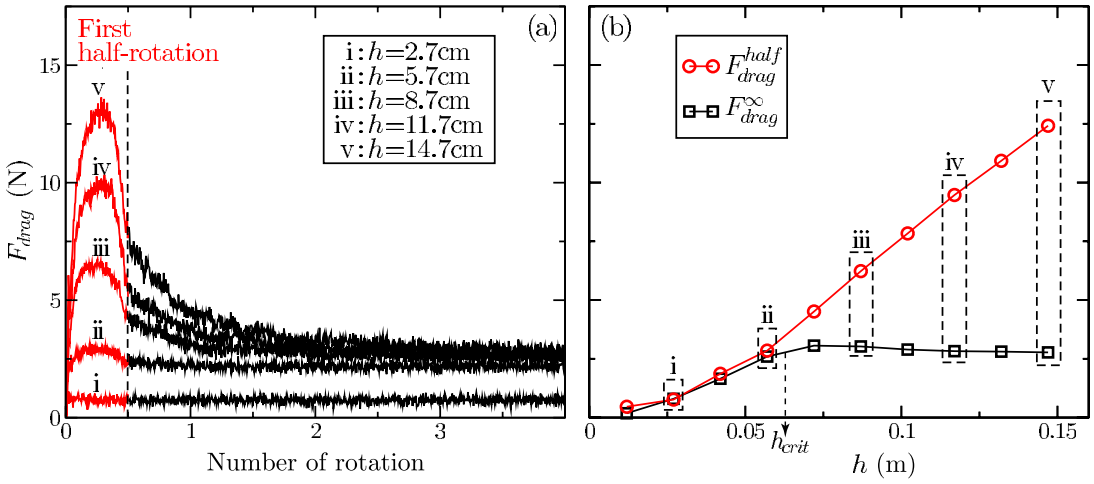

FIG. 2 (color online). (a) Drag force as a function of the number of rotations for a cylinder $D = 6$ mm, $L = 60$ mm. The different curves are obtained at different depths. The dotted line shows the end of the first half-rotation. (b) Maximum drag force during the first half-rotation ($F^{\mathrm{half}}_{\mathrm{drag}}$, red circles) and during the steady state ($F^{\infty}_{\mathrm{drag}}$, black squares) as a function of depth. The data points (i)–(v) correspond to (a).

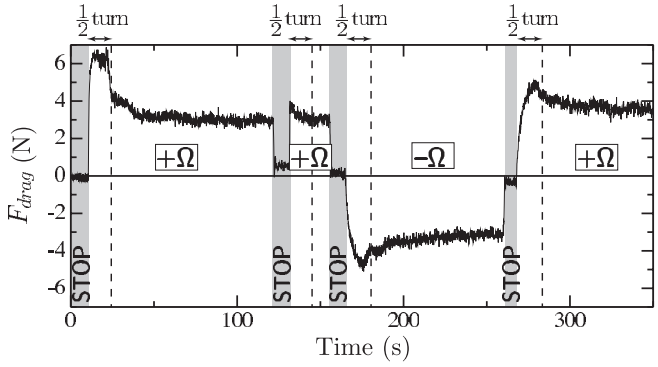

FIG. 3. Time evolution of the drag force F_{drag} when changing the rotation direction. Shaded regions correspond to rest periods. Dotted lines show the end of the first half-rotation since the last stop. $D = 6$ mm, $L = 6$ cm, $h = 12$ cm.

rod and then pouring the grains in the tank does not changes F^{∞}_{drag}. Second, stopping the rotation and/or reversing the rotation does not break the underlying structure as shown in Fig. 3. In this run the tank first rotates clockwise during several rotations and the drop of the drag after the first half turn is observed. The tank is then stopped and started again, showing almost no variation of the drag force. The tank is stopped again and the direction of rotation is reversed to counterclockwise, and back to clockwise. The peak of the drag force observed during the first half turn after starting the rotation again is much smaller than at the beginning of the run. Last, we have tried to break the structure by tapping on the tank and no effects were noticeable, showing that the structure built during the rotation is not fragile.

The observation of a depth-independent drag force raises the question of its scaling. Drag forces in granular media are usually described as a frictional phenomenon, meaning that the forces are proportional to the local confining pressure times the surface of the object. Assuming that the confining pressure is given by the hydrostatic pressure gives $F_{\text{drag}} \propto LD\rho gh$. The inset of Fig. 4 shows that this scaling holds for the drag measured during the first half-rotation. The collapse of $F^{\text{half}}_{\text{drag}}/LD$ as a function of ρgh obtained for different cylinders suggests that $F^{\text{half}}_{\text{drag}} \simeq 15LD\rho gh$, compatible with previous studies [16]. However, this classical scaling cannot hold for the stationary drag F^{∞}_{drag}, since this latter is independent of the depth h. In Fig. 4, the ratio $F^{\infty}_{\text{drag}}/LD$ in the saturated regime ($h > h_{\text{crit}}$) is plotted as a function of ρgL instead of ρgh for cylinders having different lengths. The idea is that the relevant pressure is no longer given by the depth h but by the length of the object L. The quasilinear dependence observed in Fig. 4 confirms that ρgL is the relevant pressure scale to characterize the drag. However, deviations from a strictly proportionality relation is observed at low L, as the best linear fit in Fig. 4 does not pass through

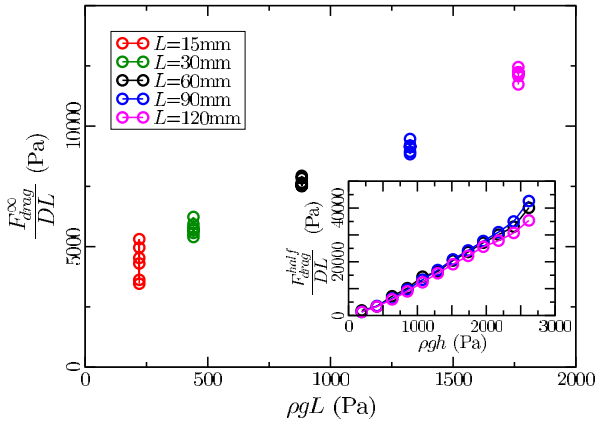

FIG. 4 (color online). Saturated drag force normalized by the cylinder surface $F^{\infty}_{\text{drag}}/DL$ as a function of ρgL ($\rho \simeq 1500$ kg/m^3) for cylinders of diameter $D = 4$ mm and various lengths L. Data for $h > h_{\text{crit}}$ only. Inset: $F^{\text{half}}_{\text{drag}}/DL$ as a function of the hydrostatic pressure ρgh.

zero. In order to more precisely determine the scaling of the drag force, we have plotted in Fig. 5(a) the ratio $F^{\infty}_{\text{drag}}/(DL\rho gL)$ as a function of the aspect ratio L/D for all cylinders. All data collapse on a single curve, which tends

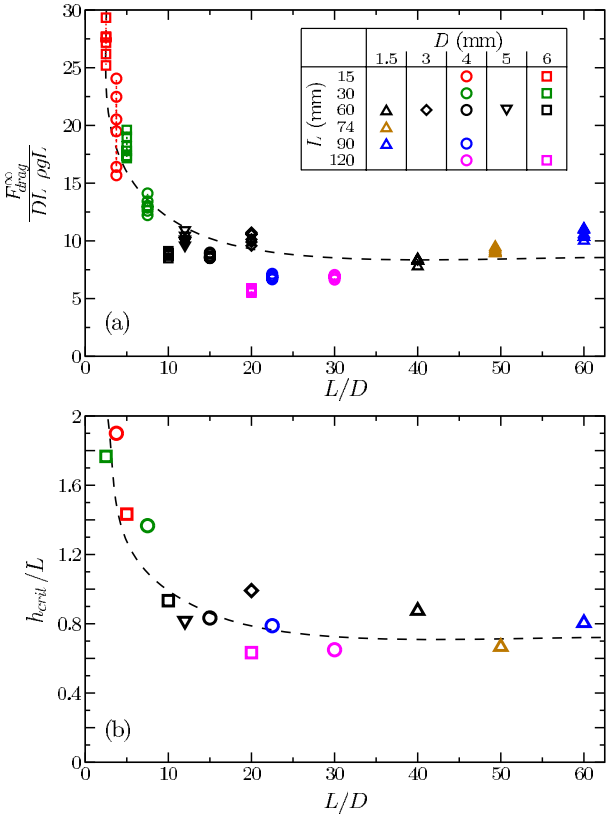

FIG. 5 (color online). (a) Dimensionless saturated drag force $F^{\infty}_{\text{drag}}/DL\rho gL$ as a function of the cylinder aspect ratio (L/D), for various cylinders. Data for $h > h_{\text{crit}}$ only. (b) Dimensionless critical depth h_{crit}/L as a function of the cylinder aspect ratio, for the same cylinders. Black dotted lines are guides for the eyes.

to a constant value at large aspect ratio: $F^{\infty}_{\rm drag}/(DL\rho gL) \simeq 10$ for $L/D \gtrsim 10$.

Our experiments, therefore, give the following scalings for the drag measured during the first half-turn and in the steady regime:

$$F^{\rm half}_{\rm drag} \simeq 15DL\rho gh, \tag{2}$$

$$F^{\infty}_{\rm drag} \simeq DL\rho gLf(L/D), \tag{3}$$

where $f(L/D)$ is a function that tends to a constant close to 10 at large aspect ratio. The expression for the stationary drag force holds only for large enough depth $h > h_{\rm crit}$. Figure 5(b) shows how the critical depth scales with the size of the cylinders. We observe that $h_{\rm crit}/L$ is a function of the aspect ratio L/D with the same shape as in Fig. 5(a). This scaling can be understood by noting that, below $h_{\rm crit}$, $F^{\infty}_{\rm drag}$ follows the hydrostatic scaling [see Fig. 2(b)]. Therefore, identifying Eqs. (2) and (3) for $h = h_{\rm crit}$ gives $h_{\rm crit} \simeq Lf(L/D)/15$, which for high aspect ratio reduces to $h_{\rm crit} \simeq 0.67L$. The pressure screening effect is then observed when the cylinder is buried at a depth larger than its length. This explains why the saturation has not been observed in previous experiments using a shallow container [16].

In the above experiments, the cylinder was kept at a constant depth. One can wonder if the screening of the hydrostatic pressure still happens when the cylinder also moves downward while rotating. The idea is to check if one can drill into a granular medium without having to develop strong torques. To this end, we perform experiments in which the cylinder is fixed on a translation stage and moves down at a constant velocity v_z between 4 and 6 mm min^{-1}, while the tank rotates at a constant angular velocity Ω between 1.5 and 2.5 rpm. The experiment being performed in the quasistatic regime, we verify that the measured drag only depends on the ratio of the velocities, which is equal to the pitch a of the helix described by the cylinder: $a = v_z/\Omega$. Figure 6 shows the time evolution of the drag force during the helicoidal motion of the cylinder for different pitches a. Two different regimes are observed. If the pitch is large (blue and purple curves), the drag force increases linearly with depth, as expected by the classical frictional argument. In this case, the cylinder is moving down too fast to feel its wake. By contrast, when the pitch a is small (black and red curves), the drag force starts to increase linearly at small h but saturates when the cylinder reaches the critical depth $h_{\rm crit}$. At each rotation, the cylinder partially goes through its wake, which seems to be sufficient to create a structure that screens the hydrostatic pressure. The critical pitch $a_{\rm crit}$ separating the two behaviors can be estimated and is plotted in the inset of Fig. 6. We observe that the critical pitch is proportional to the diameter D of the cylinder with $a_{\rm crit} \simeq 1.5D$. This is consistent with the picture of a cylinder which has to pass through its own wake in order to create a structure able

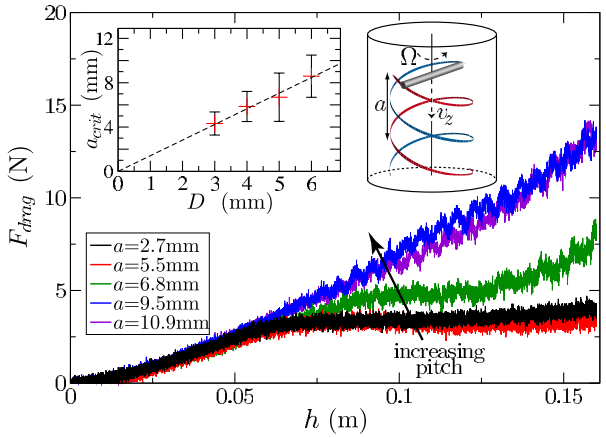

FIG. 6 (color online). Evolution of $F_{\rm drag}$ with depth during the helicoidal motion of the cylinder for different pitches a ($D = 6$ mm, $L = 6$ cm). Inset: Critical pitch $a_{\rm crit}$ as a function of the cylinder diameter D. $a_{\rm crit}$ is the average of the pitches for which the drag force for $h > h_{\rm crit}$ lies in between the hydrostatic case and the saturated case, as, for example, the green curve.

to screen the hydrostatic pressure. This experiment therefore shows that drilling into a granular medium does not necessitate strong torques, as long as the vertical motion is slow enough.

In summary, we have shown that the drag force experienced by a cylinder rotating in a granular medium becomes independent of depth, which enables us to drill inside the material with surprisingly low torques. This apparent screening of the hydrostatic pressure is reminiscent of the Janssen effect [26] observed in narrow silos, for which the pressure becomes independent of depth for depths larger than the silo width. However, the fundamental difference here is that the screening occurs without any side walls. Everything happens as if the rotating object creates its own "shield" that screens the hydrostatic pressure. It is interesting to note that a pressure screening effect has been observed in another configuration, when a sand pile is created from a funnel. The pressure under the heap presents a minimum at the center of the pile due to the orientation of the force network, reminiscent of the successive avalanches during the building of the heap [27,28]. In our case, the pressure shield likely comes from an anisotropy of the force network around the cylinder that builds during the motion and persists when the motion stops. Understanding the formation of this structure in terms of force distribution and developing continuum models able to capture this effect remain a challenge.

*francois.guillard@polytech.univ-mrs.fr
†yoel.forterre@polytech.univ-mrs.fr
‡olivier.pouliquen@univ-amu.fr

[1] D. F. James, Annu. Rev. Fluid Mech. **41**, 129 (2009).

[2] H. Tabuteau, P. Coussot, and J. R. de Bruyn, J. Rheol. **51**, 125 (2007).
[3] B. Dollet, F. Elias, C. Quilliet, C. Raufaste, M. Aubouy, and F. Graner, Phys. Rev. E **71**, 031403 (2005).
[4] Y. Forterre and O. Pouliquen, Annu. Rev. Fluid Mech. **40**, 1 (2008).
[5] K. Wieghardt, Annu. Rev. Fluid Mech. **7**, 89 (1975).
[6] T. Faug, R. Beguin, and B. Chanut, Phys. Rev. E **80**, 021305 (2009).
[7] R. D. Maladen, Y. Ding, C. Li, and D. I. Goldman, Science **325**, 314 (2009).
[8] A. G. Bengough and C. E. Mullins, J. Soil Sci. **41**, 341 (1990).
[9] R. Albert, M. A. Pfeifer, A.-L. Barabási, and P. Schiffer, Phys. Rev. Lett. **82**, 205 (1999).
[10] I. Albert, P. Tegzes, B. Kahng, R. Albert, J. G. Sample, M. Pfeifer, A.-L. Barabasi, T. Vicsek, and P. Schiffer, Phys. Rev. Lett. **84**, 5122 (2000).
[11] N. Gravish, P. B. Umbanhowar, and D. I. Goldman, Phys. Rev. Lett. **105**, 128301 (2010).
[12] B. Percier, S. Manneville, J. McElwaine, S. Morris, and N. Taberlet, Phys. Rev. E **84**, 051302 (2011).
[13] D. J. Costantino, J. Bartell, K. Scheidler, and P. Schiffer, Phys. Rev. E **83**, 011305 (2011).
[14] D. Chehata, R. Zenit, and C. R. Wassgren, Phys. Fluids **15**, 1622 (2003).
[15] I. Albert, J. G. Sample, A. J. Morss, S. Rajagopalan, A.-L. Barabási, and P. Schiffer, Phys. Rev. E **64**, 061303 (2001).
[16] T. A. Brzinski III and D. J. Durian, Soft Matter **6**, 3038 (2010).
[17] Y. Ding, N. Gravish, and D. I. Goldman, Phys. Rev. Lett. **106**, 028001 (2011).
[18] F. Zhou, S. G. Advani, and E. D. Wetzel, Phys. Rev. E **69**, 061306 (2004).
[19] D. Lohse, R. Rauhe, R. Bergmann, and D. van der Meer, Nature (London) **432**, 689 (2004).
[20] M. B. Stone, R. Barry, D. P. Bernstein, M. D. Pelc, Y. K. Tsui, and P. Schiffer, Phys. Rev. E **70**, 041301 (2004).
[21] G. Hill, S. Yeung, and S. Koehler, Europhys. Lett. **72**, 137 (2005).
[22] H. Katsuragi and D. J. Durian, Nat. Phys. **3**, 420 (2007).
[23] A. Seguin, Y. Bertho, P. Gondret, and J. Crassous, Phys. Rev. Lett. **107**, 048001 (2011).
[24] F. Pacheco-Vázquez, G. A. Caballero-Robledo, J. M. Solano-Altamirano, E. Altshuler, A. J. Batista-Leyva, and J. C. Ruiz-Suárez, Phys. Rev. Lett. **106**, 218001 (2011).
[25] S. von Kann, S. Joubaud, G. A. Caballero-Robledo, D. Lohse, and D. van der Meer, Phys. Rev. E **81**, 041306 (2010).
[26] R. M. Nedderman, *Statics and Kinematics of Granular Materials* (Cambridge University Press, Cambridge, England, 1992).
[27] L. Vanel, D. Howell, D. Clark, R. P. Behringer, and E. Clément, Phys. Rev. E **60**, R5040 (1999).
[28] J. Geng, E. Longhi, R. P. Behringer, and D. W. Howell, Phys. Rev. E **64**, 060301 (2001).